PHYSICAL REVIEW B VOLUME 3, NUMBER 8 15 APRIL 1971

Electron Transport in GaAs

D. L. Rode and S. Knight
Bell Telephone Laboratories, Murray Hill, New Jersey 07974
(Received 12 October 1970)

The electron drift mobility in GaAs has been calculated and extensively compared to experimental data. Good agreement is obtained for a wide range of temperature and ionized-impurity concentrations. Calculated results for the electron contribution to thermoelectric power are also presented and compared to the small amount of existing data. Ionized-impurity scattering, deformation-potential scattering, piezoelectric scattering, and polar scattering are included for a nonparabolic conduction band with electron-wave-function admixture. Furthermore, degeneracy has been incorporated without approximation. The formulation of electron scattering by ionized impurities is shown to fail at sufficiently low temperatures because of the loss of binary-scattering events. This feature probably obscures the expected failure of the Born approximation, given the purity of even the best present-day semiconductors.

I. INTRODUCTION

It has been shown in an earlier paper[1] that the electron drift mobility in direct-gap semiconductors can be calculated in a convenient and accurate manner by direct solution of the Boltzmann equation. Results were presented for ideally pure materials, whereas there exists a widespread need for a description of semiconductors containing varied types and concentrations of ionized impurities. The latter situation is the more common experimental one, and its detailed characterization would prove helpful in allowing a reliable impurity analysis of crystals.

The present paper is particularly concerned with n-type GaAs for which we give electron drift mobility and thermoelectric power (exclusive of phonon-drag effects[2]) as calculated for various temperatures and ionized-impurity concentrations. The mobility results are compared extensively to experimental data. Thermoelectric-power results are also given, although rather fewer experimental data are presently available. We find that the present description of transport in a single spherical-conduction-band minimum at the center of the first Brillouin zone[3] (centered about the Γ_{1c} point) is sufficient over the temperature range from 20–600 °K. Below the lower temperature, the model chosen for ionized-impurity scattering[4,5] is suspect. Above 600 °K, multivalley conduction involving satellite valleys of X_{1c} symmetry is indicated by the experimental data.

In Sec. II the matrix element for ionized-impurity scattering similar to that of Brooks and Herring[4] and of Dingle[5] is adapted to the present transport calculation. We assume the band structure given by Kane[6] for zero spin-orbit splitting of the valence bands and make no further approximation. The admixture of s- and p-type wave functions into the total electron wave function is also included. Modifications to the formulation[1] implied by the inclusion of degeneracy (i.e., Fermi statistics) are briefly stated although details of the derivation appear in another paper[7] along with formulas for thermoelectric power. Also in Sec. II we propose a combination rule which allows us to estimate the Hall-coefficient factor for several scattering mechanisms acting simultaneously when we are given the Hall-coefficient factor for each scattering mechanism acting separately.

Section III applies the formulation to a comparison between calculated and experimental results. Mobility vs temperature is given for pure material. Mobility vs free-electron concentration at 77 and 300 °K is given for several compensation ratios, as is thermoelectric power. Finally, we apply the aforementioned rule regarding Hall-coefficient factors to an analysis of mobility vs temperature for two GaAs samples exhibiting ionized-impurity scattering at low temperatures. The comparison between theory and experiment below 10 °K shows that the calculated mobilities fall well below the experimental values. The failure of the theory at these lower temperatures appears to be caused by the lack of binary-scattering events[8] by ionized impurities. The Born approximation[9] is valid for all results discussed in this paper, and it is shown that the failure of the Born approximation should not be observable until crystals of purity several orders of magnitude better than the best presently available can be obtained. In practical situations the failure of the present theory of ionized-impurity scattering is the result of the loss of binary-scattering events. At sufficiently low temperatures, higher-order processes become dominant.

II. FORMULATION

The band-structure formulation provided by Kane[6] accurately describes the shape of the lowest conduction-band minimum in GaAs. This formulation

includes the effects of higher conduction-band edges (e.g., Γ_{15c}) and spin-orbit splitting of the Γ_{15v} valence bands. However, these latter two effects provide unimportant influences (to perhaps a few percent in mobility) on electron transport.[1] Therefore, we choose the band structure and electron wave functions for zero spin-orbit splitting as discussed previously.[1]

The three most important types of lattice scattering[10] have already been incorporated[1]; these consist of scattering by acoustic modes through deformation-potential and piezoelectric interactions, and polar optical-mode scattering. We depart from Ref. 1 and include ionized-impurity scattering as well as degeneracy. Ionized-impurity scattering can ordinarily be considered elastic[4,5] so that the electron energy remains unchanged following the scattering event. In the spirit of the previous work,[1] we will incorporate these additional features without approximation so that our only assumptions are those of the band structure and the various forms of electron scattering.

The matrix element of the shielded Coulomb potential of a singly ionized center can be found in the literature.[11] The nonparabolicity of the conduction band enters as a multiplicative factor so that the differential scattering rate s_{ii} [see Eq. (13) of Ref. 1 which indicates how the differential scattering rates are to be inserted into the Boltzmann equation] for ionized-impurity scattering becomes

$$s_{ii}(\vec{k}', \vec{k}) = \frac{e^4 N}{4\pi^2 \epsilon_0^2 \hbar} \left(\frac{aa' + cc'x}{\beta^2 + |\vec{k}' - \vec{k}|^2} \right)^2 \delta(\mathcal{E}' - \mathcal{E}), \quad (1)$$

where the factor $aa' + cc'x$ accounts for nonparabolicity. The differential scattering rate $s_{ii}(\vec{k}', \vec{k})$ is the probability per unit time that an electron initially in the state characterized by $\vec{k}'$ will make a transition into the state characterized by $\vec{k}$. The crystal momentum of the electron is $\hbar\vec{k}$. N is the concentration of fixed ionized scattering centers,

$$N = N^+ + N^-, \quad (2)$$

where N^+ and N^- are the respective concentrations of ionized donor and acceptor impurities. ϵ_0 is the low-frequency dielectric permittivity. The coefficients a and c provide, respectively, the correct proportions of s- and p-type wave functions[6] for the crystal momentum state $\hbar\vec{k}$. a' and c' correspond to $\hbar\vec{k}'$. x is the cosine of the angle between $\vec{k}$ and $\vec{k}'$. $\mathcal{E}$ and $\mathcal{E}'$ are the energies of the $\vec{k}$ and $\vec{k}'$ states and the Kronecker δ function indicates that the scattering event is elastic. The quantity β is the inverse of the screening length for the Coulomb potential. In the nondegenerate limit, for example, $1/\beta$ is the Debye length. In general, however, we have

$$\beta^2 = \frac{e^2}{\epsilon_0 \kappa T} \int_0^\infty \frac{(k/\pi)^2 e^{(\mathcal{E}-\eta)/\kappa T}}{[e^{(\mathcal{E}-\eta)/\kappa T} + 1]^2} \, dk, \quad (3)$$

where κ is Boltzmann's constant and η is the Fermi energy. The electron energy $\mathcal{E}$ is, of course, a nonparabolic function of $k = |\vec{k}|$ and is given by Eq. (3) of Ref. 1. The Fermi energy derives from the band structure characterized by the effective-mass energy gap $\mathcal{E}_g^*$ and the effective mass at the band edge m^* and from the given free-electron concentration n. To calculate η, the following expression is numerically inverted:

$$n = (1/\pi^2) \int_0^\infty [k^2/(e^{(\mathcal{E}-\eta)/\kappa T} + 1)] \, dk. \quad (4)$$

The differential scattering rate, Eq. (1), must be integrated over all states $\vec{k}'$ to yield the net scattering rate S_{ii} for this process. One can show[7] that for any elastic process, the difference between the scattering-*out* rate and the scattering-*in* rate,[12] called the *scattering rate*, is precisely the usual relaxation rate,[13]

$$S_{ii} = \int (1 - x) \, s_{ii}(\vec{k}', \vec{k}) \, d\vec{k}', \quad (5)$$

$$S_{ii} = (e^4 N m d / 8\pi\epsilon_0^2 \hbar^3 k^3)[D \ln(1 + 4k^2/\beta^2) - B], \quad (6)$$

where m is the electron mass in vacuum and d accounts for the increase in effective electron mass at higher energies which is the consequence of a nonparabolic band. d is given by Eq. (5) of Ref. 1. The coefficients D and B are

$$D = 1 + 2\beta^2 c^2/k^2 + 3\beta^4 c^4/4k^4, \quad (7)$$

$$B = [4k^2 + 8(\beta^2 + 2k^2)c^2 + (3\beta^4 + 6\beta^2 k^2 - 8k^4)c^4/k^2]/(\beta^2 + 4k^2). \quad (8)$$

In the case of parabolic bands, where $c = 0$, we have $D = 1$ and $B = 4k^2/(\beta^2 + 4k^2)$, and Eq. (6) yields the previous result for Brooks-Herring scattering.[4] The scattering rate due to ionized impurities, Eq. (6), describes an elastic process and can be simply added to the scattering rates for all other elastic processes given in Ref. 1. Before we apply the above result, we should point out that the derivation of the scattering rate presumes that the scattering events are purely *binary*; i.e., the time required for the deflection of the electron by the ionized center is very small compared to the average time between collisions. Clearly, this assumption will fail at sufficiently low temperatures since the scattering rate for ionized impurities increases rapidly for decreasing temperature. To see this, we merely note that the time required for the deflection τ_D is about that necessary for the electron to travel $\sqrt{2} \times$ (screening length). For a nondegenerate semiconductor with a parabolic conduction band, we have

$$\tau_D^2 = \epsilon_0 m^*/ne^2 , \tag{9}$$

where m^* is the electron effective mass. The average time between scattering events is

$$\tau_s = m^*\mu/e , \tag{10}$$

where μ is the electron drift mobility, and we require for binary scattering that $\tau_D < \tau_s$ or

$$\mu^2 > \epsilon_0/nm^* . \tag{11}$$

We note that μ decreases as temperature decreases, and n decreases as temperature decreases, so that Eq. (11) will eventually fail at low temperatures. Equation (11) can be restated in an equivalent form which simply requires the free-electron plasma to be lightly damped, i.e.,

$$\omega_p^2\tau_s^2 > 1 , \tag{12}$$

where ω_p is the plasma frequency. Note that Eq. (11) applies only when ionized-impurity scattering is dominant. We will return to Eq. (11) in Sec. III in connection with the experimental data.

Under the influence of a small electric field, the total electron distribution function $f_T(\vec{k})$ becomes

$$f_T(\vec{k}) = f(k) + xg(k), \tag{13}$$

where f is the equilibrium Fermi-Dirac distribution and g is a small perturbation. The formula for the perturbation distribution g has been derived elsewhere[7] (the same notation has been followed in this reference), with the result that g is given by a finite difference equation. This finite difference equation has been solved numerically by iteration, as previously.[1] The convergence is rapid so that about four iterations suffice for an accuracy of 1%. From g, the drift mobility follows directly.[1]

For the measurement of thermoelectric power Q, one applies a small temperature gradient ∇T to an open-circuited sample of material.[2] The diffusion of free carriers along the gradient develops an electric field. The ratio of electric field to temperature gradient equals Q. The details of the calculation of Q can be found in Ref. 7. We shall only state the results applicable to GaAs in Sec. III.

Since nearly all experimental data for mobility are, in fact, Hall mobilities rather than drift mobilities as are calculated here, we need to estimate the correction on this account. The Hall effect yields the free-electron concentration to within a factor which is called the Hall-coefficient factor r_H (usually between unity and two).[14] Henceforth, we refer to r_H as the Hall factor and to a mobility derived by the common assumption that $r_H = 1$ as a Hall mobility μ_H. The quantity r_H is known for various scattering mechanisms acting *independently* and especially for elastic processes. These are given in Table I (r_H is calculated from Ref. 4).

TABLE I. Hall factors.

Scattering mechanism	Hall factor[a]
Acoustic modes, deformation potential	$r_H = 3\pi/8 = 1.18$
Acoustic modes, piezoelectric	$r_H = 45\pi/128 = 1.10$
Ionized-impurity centers[b]	$r_H = 315\pi/512 = 1.93$
Polar-optical modes	See Refs. 15–18.

[a] r_H is calculated for a parabolic conduction band.
[b] S_{ii} is assumed proportional to $1/k^3$.

Various calculations[15–17] have been made of r_H for polar-mode scattering, the only inelastic scattering process with which we are concerned, and we choose to use those of Ref. 15 in view of recent experiments.[18] Even though the various calculations disagree considerably, the correction on this account is generally less than 30%, so that our over-all error in mobility should be less than 15%. Of course, the various scattering mechanisms act simultaneously and sometimes several are of equal importance in practice. Hence we need a method by which to estimate the combined Hall factors. No rule for this purpose appears to be available so that we will construct the following combination rule. We first assume Matthiessen's rule

$$1/\mu = \sum_i 1/\mu_i , \tag{14}$$

where μ is the *drift* mobility and the μ_i are component *drift* mobilities for each scattering mechanism acting alone. Next, we postulate that

$$1/r_H\mu \equiv 1/\mu_H = \sum_i 1/\mu_{Hi} \equiv \sum_i 1/r_{Hi}\mu_i , \tag{15}$$

where the μ_{Hi} are the component Hall mobilities and the r_{Hi} are the corresponding Hall factors. Combining Eqs. (14) and (15) leaves

$$r_H = \frac{\sum_j 1/\mu_j}{\sum_j 1/r_{Hj}M_j} , \tag{16}$$

which allows us to calculate the over-all Hall factor r_H given the r_{Hi} and the drift mobilities. Of course, Eq. (15) is not strictly true, in general, but mobility errors thereby incurred are of second order so that Eq. (16) should still be a useful formula. We note only that Eq. (15) is true if Matthiessen's rule is true. Because Eq. (15) cannot be proven from Eq. (14), it must be regarded as an independent assumption. We will apply this rule in Sec. III to comparisons between calculated drift mobilities and experimental Hall mobilities.

III. RESULTS

There are several material parameters (e.g., effective mass, energy gap, etc.) required for the calculation. The values of these parameters are tabulated in Ref. 1 and those are the values used

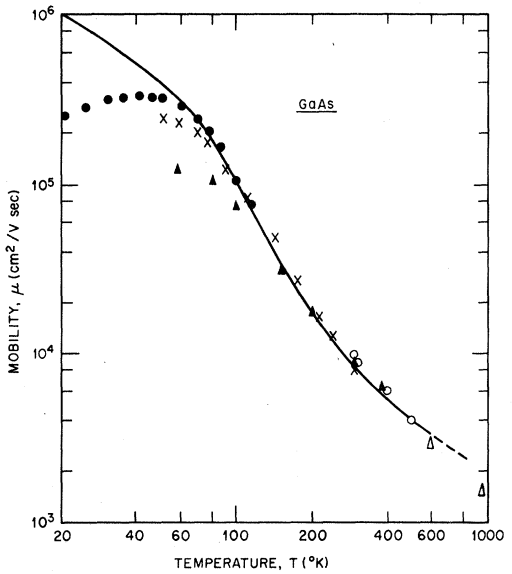

FIG. 1. Electron drift mobility of pure (intrinsic) GaAs vs temperature. The solid curve is calculated. The dashed portion of the curve above 600 °K indicates the onset of multivalley conduction which is not included in the present formulation. The data points represent measured Hall mobilities: ● , Ref. 21; ×, Ref. 22; ▲, Ref. 23; ○ , Ref. 24; △, Ref. 25.

here, with the exception of the acoustic deformation potential E_1. In accordance with the sequence of values of E_1 for II-VI semiconductors, and, in particular, that found for ZnSe (11.5 eV),[19] we choose $E_1 = 11.5$ for the present calculations. In addition, some calculations are presented below for $E_1 = 7$ eV (indicated on the figures), as found by Ehrenreich,[20] and we must conclude that it is not now possible to decide with certainty which of these two values is preferable. Given the various remaining parameters as determined by independent experiments, the mobility can be calculated with no adjustable parameters.

The electron drift mobility in pure (intrinsic) GaAs vs temperature appears in Fig. 1. The solid line represents calculated values and the data points are taken from various experiments[21-25] (see the figure caption). Above 600 °K the calculated curve is dashed since the high-temperature data of Smith[25] as well as approximate calculations of our own indicate the onset of multivalley conduction at this temperature. These additional valleys are three in number and are probably centered at the X_{1c} points of the first Brillouin zone.[10,26] The X_{1c} minima lie 0.3–0.4 eV above the very nearly spherical Γ_{1c} minimum. Below 600 °K and down to 100 °K, the mobility is dominated by polar-mode scattering. Near 80 °K, piezoelectric and deformation-potential acoustic-mode scattering become as important as polar-mode scattering. Below 60 °K, piezoelectric scattering remains the dominant lattice scattering mechanism. The experimental data confirm the calculated curve from 60–600 °K. Below 60 °K even the purest material discussed here[21] shows a decreasing mobility with decreasing temperature. Such behavior is, of course, symptomatic of ionized-impurity scattering and is discussed in detail later (see Fig. 6 and 7). The calculated electron drift mobility for pure GaAs is 7900 cm²/V sec at 300 °K and 194 000 cm²/V sec at 77 °K. From the combination rule for the Hall factor, Eq. (16), we estimate corresponding Hall mobilities of 8400 cm²/V sec at 300 °K and 219 000 cm²/V sec at 77 °K. These latter values agree well with the respective experimental values of 8200–8900 cm²/V sec[22] and ~ 200 000 cm²/V sec[21] for the purest available materials.

Oftentimes, it is desirable to know the mobility for certain concentrations of donor and acceptor impurities. These data are helpful not only for predicting mobility under specific conditions of doping, but also for estimating impurity concentrations by analyzing Hall data. Since Hall data do give reasonable estimates of free-carrier concentration and drift mobility (aside from the Hall factor), we have plotted in Figs. 2 and 3, μ vs n at 300 and 77 °K. The calculated curves are plotted for several values of compensation ratio, defined as

$$\frac{\text{concentration of fixed ionized centers}}{\text{concentration of mobile charges}} = \frac{N^+ + N^-}{n} .$$

For perfectly pure (intrinsic) material, the compensation ratio includes the free-hole concentration p so that $(N^+ + N^-)/(n+p) = 0$, but for ideal extrinsic n-type material (no acceptors), where p is negli-

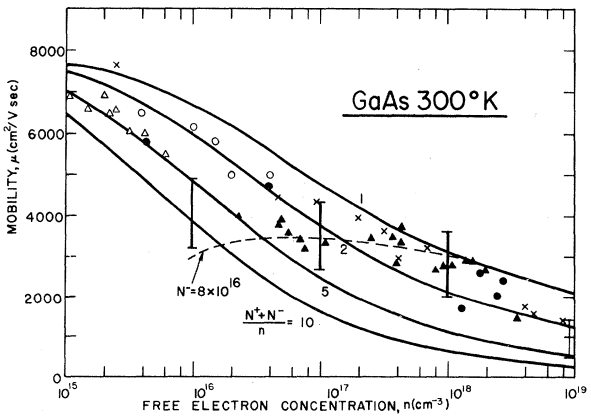

FIG. 2. Electron drift mobility vs free-electron concentration at 300 °K. The curves are calculated for compensation ratios of 1, 2, 5 and 10. Experimental Hall mobilities appear as data points: ×, Ref. 23; △, Ref. 27; •, Ref. 28; ○ , Ref. 29; I, Ref. 30; ▲, Ref. 31.

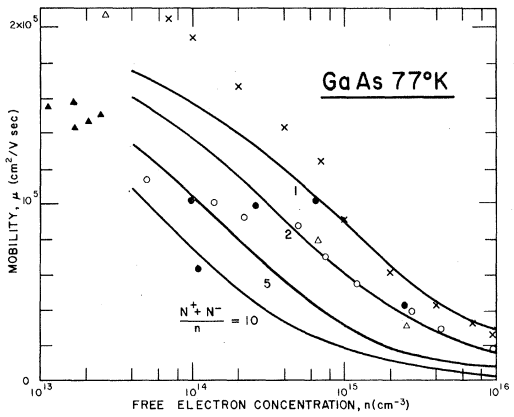

FIG. 3. Electron drift mobility vs free-electron concentration at 77 °K. The curves are calculated for compensation ratios of 1, 2, 5, and 10. Experimental Hall mobilities appear as data points: △, Ref. 18; ▲, Ref. 22; ●, Ref. 23; ×, Ref. 32; ○, Ref. 33.

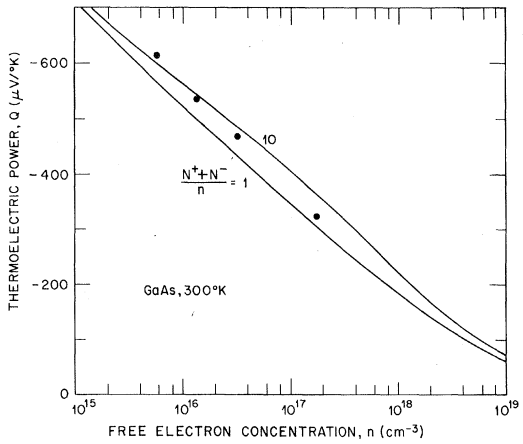

FIG. 4. Thermoelectric power vs free-electron concentration at 300 °K. The curves are calculated for compensation ratios of 1 and 10. Experimental data are from Emelyanenko *et al.* (Ref. 34).

gible, the compensation ratio becomes unity. This latter case corresponds to the upper curve in each of Figs. 2 and 3. The various points in the figures are Hall mobilities (we ignore the Hall-factor corrections here) from several experiments,[22,23,27-33] as indicated in the figure captions. The vertical bars[30] and the solid triangles[31] in Fig. 2 are data taken from the brochures of two commercial suppliers of GaAs. We note that the derived compensation ratios suggest acceptor concentrations of $(5-10)\times10^{16}$ cm^{-3} even in the n-type materials. The dashed curve illustrates a μ-vs-n curve for a fixed acceptor concentration of 8×10^{16} cm^{-3}.

The data points of Wolfe *et al.*[32] (derived for $N^-=0$ from Fig. 3 of Ref. 32) in Fig. 3 fall above the highest curve for mobility. The discrepancy may arise from the Hall factor which always causes the Hall mobility to exceed the drift mobility. For $n>10^{15}$ cm^{-3}, these same data[32] agree well with the calculated curve. This behavior may seem peculiar since r_H should be near unity when $\mu B\gg1$. $B=5$ kG for these data[32] and so μB is greater at low n than at high n, whereas the good agreement occurs at high n (above 10^{15} cm^{-3}). On the other hand, when impurity scattering becomes dominant at high n, the mobility μ in an uncompensated sample is inversely proportional to n. Therefore, even though n is underestimated by the assumption that $r_H=1$, the mobility is overestimated by a corresponding amount and no discrepancy should appear at high values of n on a μ-vs-n plot. The remaining data in Fig. 3 confirm the expected behavior that high-compensation ratios accompany low values of free-electron concentration.

Regarding the importance of including degeneracy, we mention that the neglect of degeneracy overestimates the mobility at room temperature when $(N^++N^-)/n=1$ by 25% for $n=5\times10^{18}$ cm^{-3} and by 65% for $n=10^{19}$ cm^{-3}. In fact, the neglect of degeneracy for $n>2\times10^{18}$ cm^{-3} leads to the absurd prediction that μ actually *increases* with increasing n. Such behavior can be ascribed to a rapid decrease in scattering rate which follows from Eq. (6) in the limit of large free-electron concentration. We also note that the Born approximation[9] fails in this limit, although for *all* cases described in this paper (Figs. 1–7) the Born approximation *is* valid.

Figures 4 and 5 present the thermoelectric power Q vs n at 300 and 77 °K. Phonon-drag effects[2] are not included and should not be important at 300 °K, although some complication on this account may arise at 77 °K. The authors were successful in discovering only the few experimental data points of Emelyanenko *et al.*[34] shown in Fig. 4.

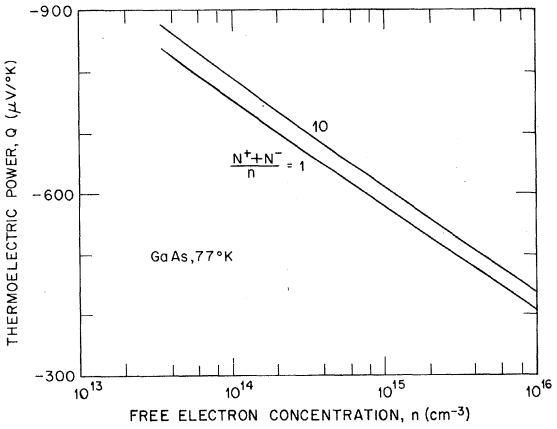

FIG. 5. Thermoelectric power vs free-electron concentration at 77 °K. The curves are calculated for compensation ratios of 1 and 10.

The last two figures, 6 and 7, illustrate typical experimental results for Hall mobility vs temperature. These two samples[18,23] are quite pure, however, with $N \approx 10^{15}$ cm^{-3} in both cases. The actual values of N^+ and N^- were derived independently of mobility from Hall-statistics analyses by the experimenters[18,23] and these derived values were used without modification in the present mobility calculations. (We assume the acceptor energy levels to be low lying so that N^- remains constant over the full range of temperature.) The solid curves are calculated for acoustic deformation-potential values of 7 and 11.5 eV. The difference between the two curves is not sufficiently great to warrant a preference for either one over the other. The vertical bars represent the experimental data, but the vertical lengths of the bars do *not* correspond to accuracy estimates. We have placed the experimental values of Hall mobility at the upper ends of the bars. The lower ends of the bars correspond to *drift* mobilities where Eq. (16) was used to derive the Hall factor. For example, ionized-impurity scattering dominates at the lowest temperatures, and the lengths of the bars indicate the factor $r_H = 1.93$ (see Table I). The true experimental drift mobilities should lie somewhere along the lengths of the bars since μB varies above and below unity for the temperature ranges of Figs. 6

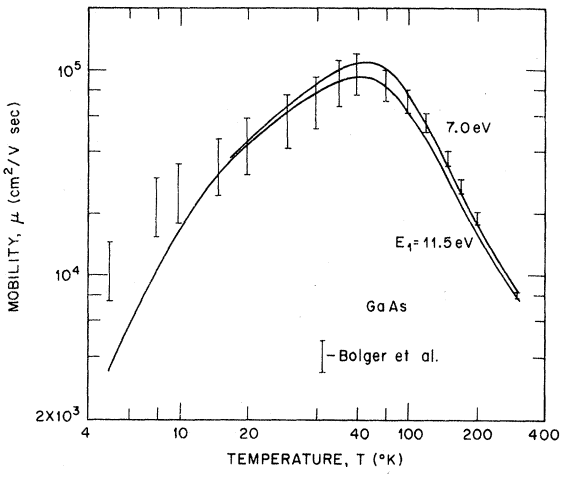

FIG. 6. Electron drift mobility vs temperature including ionized-impurity scattering. The curves are calculated for acoustic-deformation potentials of 7 and 11.5 eV. Experimental data by Bolger *et al.* (Ref. 23) from Hall-statistics analyses yield the values of n and N^- used in the calculations. The upper ends of the vertical bars correspond to measured Hall mobilities (Ref. 23) and the lower ends of the bars are calculated lower limits to the corresponding drift mobilities. The true drift mobility lies somewhere along the length of a given bar; $N^+ = 6.1 \times 10^{14}$ cm^{-3} and $N^- = 3.5 \times 10^{14}$ cm^{-3} at room temperature (Ref. 23).

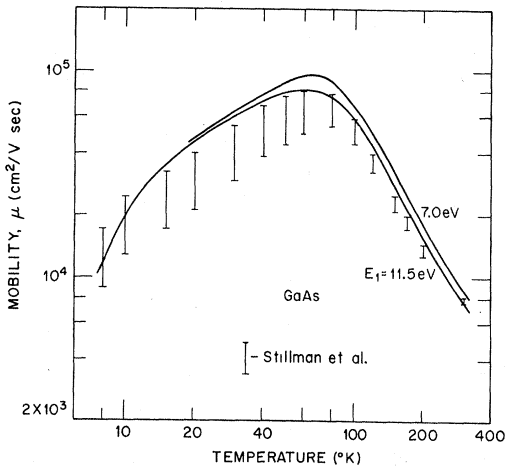

FIG. 7. Identical to Fig. 6 except that the experimental data are taken from Stillman *et al.* (Ref. 18); $N^+ = 1.1 \times 10^{15}$ cm^{-3} and $N^- = 3.3 \times 10^{14}$ cm^{-3} at room temperature (Ref. 18).

and 7. $B = 5.1$ kG[23] for the data of Fig. 6, and $B = 5$ kG[18] for the data of Fig. 7. Although Matthiessen's rule has not been used in the calculation of mobility, we wish to illustrate the danger of its use in connection with μ-vs-T plots. Calling μ_m the drift mobility derived from Eq. (14), the calculated ratio μ_m/μ is presented in Table II for the experimental data appearing in Figs. 6 and 7. Note that μ_m overestimates the drift mobility by more than 30% at 100 °K.

The agreement between theory and experiment in Fig. 6 is fair for temperatures greater than 20 °K. It appears that the impurity concentrations quoted[18] for the data shown in Fig. 7 may be somewhat low since the calculated curves lie too high. In any case, a lowering of the curves in Fig. 7 to achieve coincidence with experiment would show that the calculated mobility below 10 °K is too low. Figure 6 shows more clearly a similar discrepancy below 10 °K. We believe this appearance of failure to be attributable to the formulation of ionized-impurity scattering as discussed in Sec. II. The Born approximation at 10 °K is well satisfied, but we note that Eq. (11) is violated between 10 and 20 °K. The respective free-electron concentrations at 10 and 20 °K are[23] 1.4×10^{13} cm^{-3} and 1.35×10^{14} cm^{-3} for the sample of Fig. 6. The measured Hall mobility[23] gives $\mu_H^2 = 12$ m^4/V^2 sec^2 at 10 °K and 33 m^4/V^2 sec^2 at 20 °K for Fig. 6, whereas the respective values of ϵ_0/nm^* [see Eq. (11)] are 137 and 14. The latter values 33 and 14 satisfy Eq. (11), and the former values violate it. At even lower temperatures the ionized-impurity scattering events bear still less resemblance to the binary process required by the present formulation. Since the deflection time for an electron undergoing a scattering event is greater

TABLE II. Accuracy of Matthiessen's rule.

T(°K)	μ_m/μ (data from Ref. 23)	μ_m/μ (data from Ref. 18)
10	1.00	1.00
20	1.02	1.02
40	1.11	1.10
60	1.24	1.21
80	1.34	1.34
100	1.35	1.37
120	1.30	1.32
150	1.22	1.24
200	1.12	1.15
300	1.04	1.07

than the average time between scattering events, the electron senses the presence of several scattering centers simultaneously. At these low temperatures the material is highly compensated so that the scattering centers consist of positive as well as negative charges. This hybrid complex of charges of both polarities would be expected to be less effective at scattering than the same number of isolated charges so that, as in Figs. 6 and 7, the measured mobility should exceed the calculated values.

The criterion for satisfaction of the Born approximation[9] depends upon large values of $k^2/\beta^2 \sim T^2/n$ in the nondegenerate case which we have at hand. Similarly, Eq. (11) concerning the existence of binary scattering relies upon large values of $n\mu^2 \sim T^3/n$ for uncompensated material (the inclusion of compensation strengthens the argument). The criterion for binary scattering fails more rapidly with decreasing temperature than the criterion regarding the Born approximation (as T^3 in the former case and as T^2 in the latter case). Therefore, far purer materials than those presently available are necessary if one wishes to observe the failure of the Born approximation. Although we mentioned 20 °K in Sec. I as a lower temperature limit for application of the present results, it is now clear from Eq. (11) that this limit depends upon n when impurity scattering is important. For pure lattice scattering, previous results[19] indicate that the present description should suffice down to, and perhaps somewhat below 2 °K.

Note added in proof. The experimental data of Wolfe *et al.*[32] which exceed the uppermost curve in Fig. 3 were inaccurately collected by one of us (D. L. R.), and the subsequent assistance of Dr. Wolfe has shown Ref. 32 and Fig. 3 to be in excellent agreement. The present work has also been extended to the Hall effect for finite magnetic field, and these results lead to only slight alterations of detail. In particular, the agreement with experiment in Fig. 7 is in concordance with the estimated 20% accuracy in impurity concentrations personally communicated to the authors by Dr. Stillman.[18]

[1]D. L. Rode, Phys. Rev. B 2, 1012 (1970).

[2]C. Herring, Phys. Rev. 96, 1163 (1954).

[3]The band structure of GaAs has been calculated by, among others, D. Jones and A. H. Lettington [Solid State Commun. 7, 1319 (1969)] and reviewed by M. Balkanski and E. Amazallag [Phys. Status Solidi 30, 407 (1968)].

[4]H. Brooks, Advan. Electron. Electron Phys. 7, 85 (1955); C. Herring (unpublished).

[5]R. B. Dingle, Phil. Mag. 46, 831 (1955).

[6]E. O. Kane, J. Phys. Chem. Solids 1, 249 (1957).

[7]D. L. Rode (unpublished).

[8]The assumption of binary-scattering events is equivalent to the assumption that the time required for the electron to be deflected by the scattering potential is much smaller than the average time lapsed between scattering events.

[9]Satisfaction of the Born approximation requires that the crystal-momentum wave number k be much larger than the inverse screening length of the scattering potential.

[10]H. Ehrenreich, J. Appl. Phys. Suppl. 32, 2155 (1961).

[11]H. Ehrenreich, J. Phys. Chem. Solids 9, 129 (1959).

[12]The terms "scattering *in*" and "scattering *out*" refer to probability fluxes for scattering *into* and *out of* differential volume elements in momentum space. These terms are discussed in Ref. 1.

[13]Equation (5) prescribes the most common method of deriving the relaxation rate, wherein a weighting factor $1-x$ is included.

[14]E. Burstein and P. H. Egli, Advan. Electron. Electron Phys. 7, 59 (1955).

[15]B. F. Lewis and E. H. Sondheimer, Proc. Roy. Soc. (London) A227, 241 (1954).

[16]S. S. Devlin, *Physics and Chemistry of* II-VI *Compounds*, edited by M. Aven and J. S. Prener (Wiley, New York, 1967), p. 561.

[17]A. Fortini, D. Diguet, and J. Lugand, J. Appl. Phys. 41, 3121 (1970).

[18]G. E. Stillman, C. M. Wolfe, and J. O. Dimmock, J. Phys. Chem. Solids 31, 1199 (1970).

[19]D. L. Rode, Phys. Rev. B 2, 4036 (1970).

[20]H. Ehrenreich, J. Phys. Chem. Solids 2, 131 (1957).

[21]C. M. Wolfe, G. E. Stillmann, and W. T. Lindley, J. Appl. Phys. 41, 3088 (1970).

[22]H. G. B. Hicks and D. F. Manley, Solid State Commun. 7, 1463 (1969); and D. F. Manley (private communication).

[23]D. E. Bolger, J. Franks, J. Gordon, and J. Whitaker, in *Proceedings of the International Symposium on GaAs Reading*, 1966 (The Institute of Physics and the Physical Society, London, 1967), p. 16.

[24]D. M. Chang, privately communicated by J. Barrera.

[25]F. T. J. Smith (private communication).

[26]G. D. Pitt and J. Lees, Solid State Commun. 8, 491 (1970).

[27]F. J. Reid and L. B. Robinson, in *Proceedings of the International Symposium on GaAs, Dallas*, 1968 (The Institute of Physics and the Physical Society, London, 1969), p. 59.

[28]S. J. Bass and P. E. Oliver in Ref. 23, p. 41.

[29]A. R. Goodwin, C. D. Dobson, and J. Franks, in Ref. 27, p. 36.

[30]Commercial supplier No. 1 (unpublished).
[31]Commercial supplier No. 2 (unpublished).
[32]C. M. Wolfe, G. E. Stillman, and J. O. Dimmock, J. Appl. Phys. 41, 504 (1970).
[33]R. Solomon, in Ref. 27, p. 11.
[34]O. V. Emelyanenko, D. N. Nasledov, V. G. Sidorov, V. A. Skripkin, and G. N. Talalakin, Phys. Status Solidi 12, K93 (1965).

PHYSICAL REVIEW B VOLUME 3, NUMBER 8 15 APRIL 1971

Dielectric Screening in a Layered Electron Gas

P. B. Visscher and L. M. Falicov
Department of Physics, University of California, Berkeley, California* 94720
(Received 13 October 1970)

A model anisotropic system, suggestive of the graphite structure, is investigated: It consists of a series of equally spaced parallel planes. A finite two-dimensional density of electrons in each plane is allowed to move freely in the plane, but tunneling between planes does not take place. The dielectric screening of a point charge is evaluated exactly in the random-phase approximation. For realistic electron densities and interlayer separations the screened potential drops off very rapidly both in the plane of the charge and perpendicular to it. The induced charge density is determined, and validity of the Thomas-Fermi approximation is discussed.

I. INTRODUCTION

In this paper we calculate the screening properties of a model anisotropic system, chosen for its resemblance to the graphite structure. The system consists of electrons constrained to move on parallel equally spaced planes; the single-particle states in the absence of interactions are two-dimensional plane waves.

The screening properties are investigated by calculating the dielectric response of the system to an external point charge on one of the planes. We use the self-consistent-field dielectric formulation of Ehrenreich and Cohen, [1] which is equivalent to the random-phase approximation (RPA). We introduce an infinitesimal perturbation V^{ext} (taken to be e^2/r), compute the induced potential V^{ind} owing to the density fluctuations caused by some total potential V^{tot}, and solve $V^{\text{tot}} = V^{\text{ext}} + V^{\text{ind}}$ for V^{tot}.

It is of interest to see whether there is a strong anisotropy in the screening, with the total potential decreasing at very different rates in the plane of the test charge and perpendicular to it. It is found that, in spite of the extreme anisotropy of the model, the screening lengths are comparable, and only under very extreme conditions is such strongly anisotropic screening found.

II. DERIVATION OF SELF-CONSISTENT-FIELD EQUATIONS

Consider a system of noninteracting electrons moving in a potential which depends only on z and has very narrow deep potential wells centered around $z = 0, \pm c, \pm 2c, \ldots$. For purposes of normalization assume $\vec{r} \equiv (x, y)$ is confined to a region of area A. The unperturbed eigenstates will then have wave functions

$$\psi_{\vec{k},\sigma,m}(\vec{r}, z) = A^{-1/2} a_\sigma e^{i\vec{k}\cdot\vec{r}} \chi(z - mc),$$

where $\vec{k}$ is a two-dimensional vector, the integer m labels the planes, and a_σ is a spin eigenfunction.

We consider only the limit in which the wells are arbitrarily deep and narrow, so that only the lowest one-dimensional eigenstate $\chi(z)$ can be occupied by an electron of finite energy. $\chi(z)$ is then effectively the square root of a δ function; that is, it is arbitrarily highly localized and

$$\int_{-\epsilon}^{\epsilon} \chi^2(z)\, dz = 1$$

for any $\epsilon > 0$.

Except for the energy contribution due to χ (which is the same for all states), the unperturbed eigenvalues are

$$E_{\vec{k},\sigma,m} = E_{\vec{k}} = (\hbar^2/2m_e)k^2 .$$

Assume the system is in its unperturbed (noninteracting) ground state, with a two-dimensional "Fermi disk" of radius k_F, where

$$An = \sum_{|\vec{k}| < k_F} 2 = \frac{2A}{(2\pi)^2}\, \pi k_F^2 .$$

Thus the density of electrons (per unit area) n is

$$n = k_F^2/2\pi .$$

The one-particle density matrix is then

$$\rho_0 = \sum_{\substack{|k| < k_F \\ \sigma, m}} |\vec{k}, \sigma, m\rangle\langle\vec{k}, \sigma, m| = \sum_s f_s |s\rangle\langle s| ,$$

where $s = (\vec{k}, \sigma, m)$ and f_s is the occupation number.